Supporting Information

Nickel oxide@nickel-graphene quantum dot self-healing hydrogel for colorimetric detection and removal of lambda-cyhalothrin in kumquat

Nana Li[a], Ruiyi Li[b], Guangli Wang[a], Haiyan Zhu[a] and Zaijun Li[a*]

[a:] *Key Laboratory of Synthetic and Biological Colloids, Ministry of Education, School of Chemical and Material Engineering, Jiangnan University, Wuxi 214122, China*

[b:] *School of Pharmaceutical Science, Jiangnan University, Wuxi 214122, China*

1. Experimental

1.1 Materials and reagents

Citric acid, histidine, nickel chloride, sodium acetate, acetic acid, sodium tetraborate, poly(vinyl alcohol) (PVA, Mw 75000) and other reagents employed were all of the highest analytical grade or quality reagents purchased from Shanghai Chemical Company (Shanghai, China). 3,3',5,5'-tetramethylbenzidine (TMB) was purchased from Sigma-Aldrich (Mainland, China). Lambda-cyhalothrin and other pesticide standards were bought from Dr. Ehrenstorfer Gmbh (Augsburg, Germany). Histidine-functional graphene quantum dot (His-GQD) was prepared by using the reported method [1]. The acetate buffer solution (0.1 M, pH 3.5) was prepared by the laboratory. Ultrapure water (18.2 MΩ cm) purified from a Milli-Q purification system was used throughout the experiment.

1.2. Apparatus

Transmission electron microscopy (TEM) imaging was conducted on a JEOL-2010 FEG microscope at an acceleration voltage of 200 kV (JEOL, Japan). X-ray photoelectron spectroscopy (XPS) measurement was performed using a PHI 5700 ESCA spectrometer (Kratos, England). X-ray diffraction (XRD) pattern was measured on X-ray D8 Advance Instrument operated at 40 kV and 20 mA, using Cu-Kα radiation source with λ=0.15406 nm. Infrared spectra (IR) were recorded on a Nicolet FT-IR 6700 spectrometer (Thermo Fisher Scientific, America). Rheology data were obtained on a DHR-3 Rheometer (TA, America). The micrographs were taken using a VHX-

1000C super depth of field three-dimensional microscope (Keyence, Hong Kong). UV-diffuse reflectance spectrum were collected by a UV–vis–NIR spectrometer (Hitachi UV-3600 plus) with $BaSO_4$ as the background. UV-visible spectra were recorded on UV-2700 spectrometer (Shimadzu, Japan).

1.3. NiO and NiO@Ni preparation

NiO and *NiO@Ni* were prepared according to the methods reported in the previous literature [2]. In a typical procedure, nickel nitrate (0.1 M) and urea solution (0.1 M)were added to the round-bottomed flask at a volume ratio of 1:4, and reacted at 100°C for 10 h. After cooling to room temperature, it was orderly treated by centrifugation at 5000 rpm for 1 min, wash with deionized water and ethanol three times until the supernatant becomes neutral, drying overnight at 60°C. NiO was annealed in air at 600°C for 2 h with a heating rate of 1°C min-1. NiO@Ni was heated at 600°C in N2 for 2 h and then oxidized in air at 200°C for 30 min.

1.3. Oxidase-mimic activity measurement

NiO@Ni-His-GQD (100 μL, 1 mg mL^{-1}) dispersion or other catalyst solution was added into a mixture of TMB (100 μL, 10 mM) and acetate buffer (800 μL, pH 4.0) and stirred under vortex oscillation for 1 min. To study the oxidase-mimic activity of NiO@Ni-His-GQD, the absorbance at 652 nm of reaction solution was measured on the spectrophotometer.

The steady-state kinetic behavior of NiO@Ni-His-GQD for the oxidation of TMB was studied by changing the concentration of TMB. The kinetic parameters were obtained from the double reciprocal form of Michaelis-Menten equation: Lineweaver-Burk model (1) [3], where V is the initial velocity, V_{max} is the maximum reaction velocity, [S] corresponds to the substrate concentration, and K_M is Michaelis constant. Firstly, the absorbance values at 652 nm at different reaction times were measured. Then, the absorbance values were substituted into Lambert-beer formula to calculate the concentration of ox-TMB. The molar absorption coefficient of ox-TMB is 39000 M^{-1} cm^{-1} at 652 nm. The initial reaction rate V of different reaction systems is equal to the ratio of the corresponding ox-TMB concentration to the reaction time. According to V value of the reaction system, V_{max} and K_M can be calculated by Lineweaver-Burk equation.

$$\frac{1}{V} = \frac{K_M}{V_{max}} \cdot \frac{1}{[S]} + \frac{1}{V_{max}} \qquad (1)$$

2. Figures

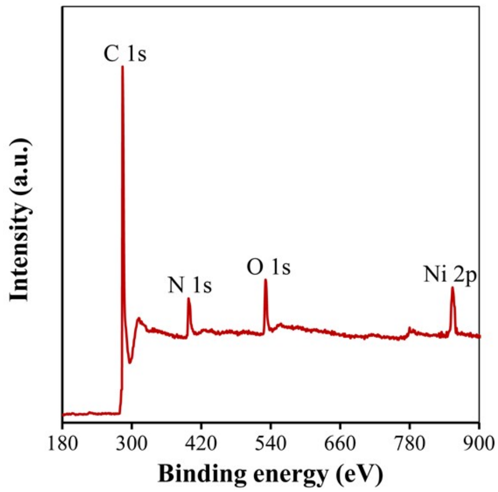

Fig. s1 XPS wide survey sprctra of NiO@Ni-His-GQD

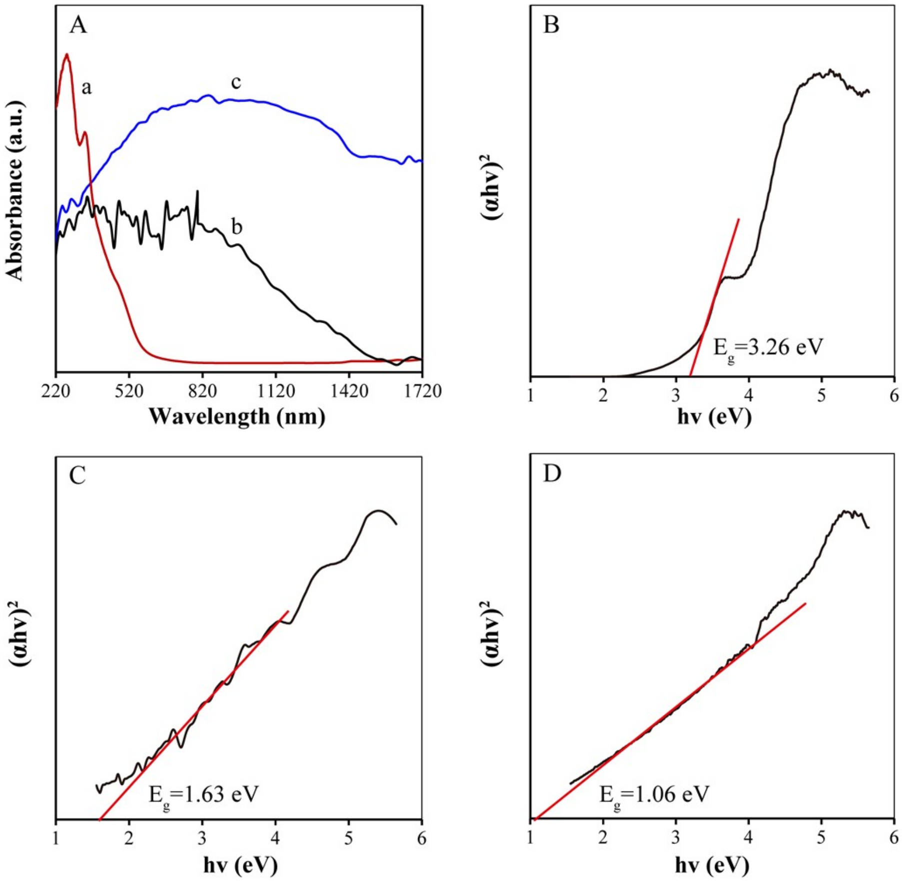

Fig. s2 UV-vis-NIR absorption spectra (A) of His-GQD (a), NiO (b), and NiO@Ni-His-GQD (c),and the plots of $(\alpha h\nu)^2$ vs. hν for the band gap energy of His-GQD (B), NiO (C) and NiO@Ni-His-GQD (D)

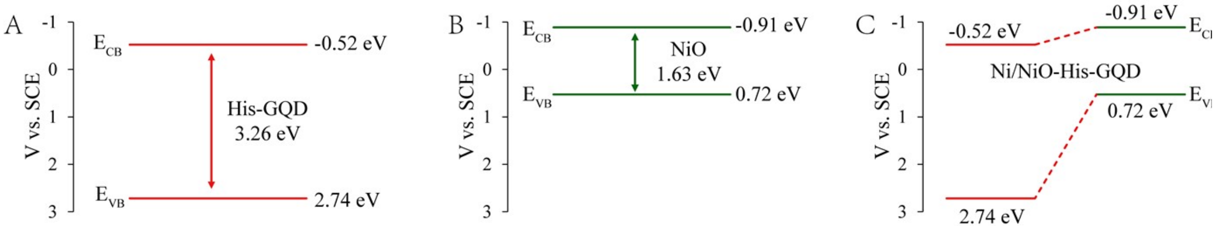

Fig. s3 The energy band diagrams of His-GQD (A), NiO (B), and NiO@Ni-His-GQD (C)

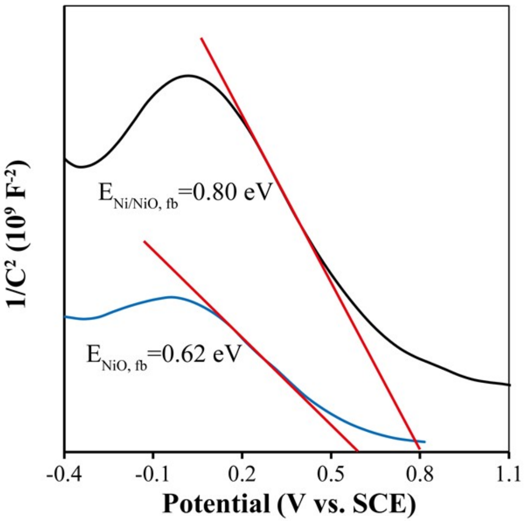

Fig. s4 The Mott-Schottky plots of NiO and NiO@Ni

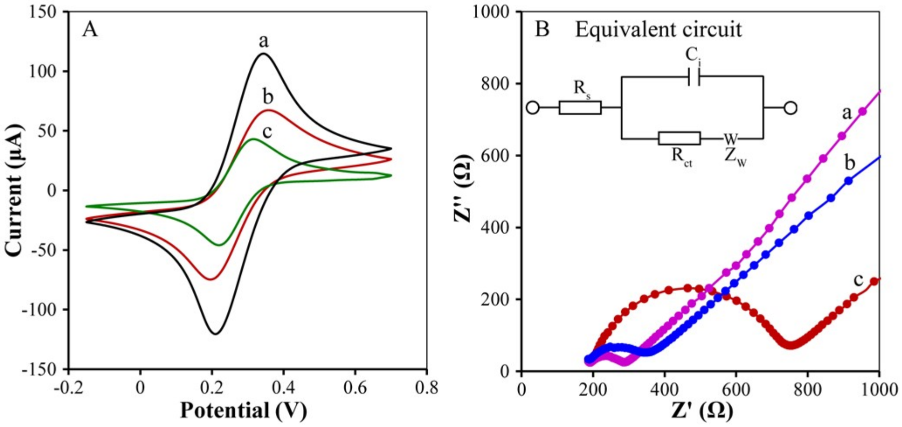

Fig. s5 Cyclic voltammetry (A) and electrochemical impedance spectroscopy (B) curves of NiO@Ni-His-GQD (a), NiO@Ni (b) and His-GQD (c) modified glassy carbon electrode in the PBS of 7.0 containing 5.0 mM $[Fe(CN)_6]^{3-/4-}$

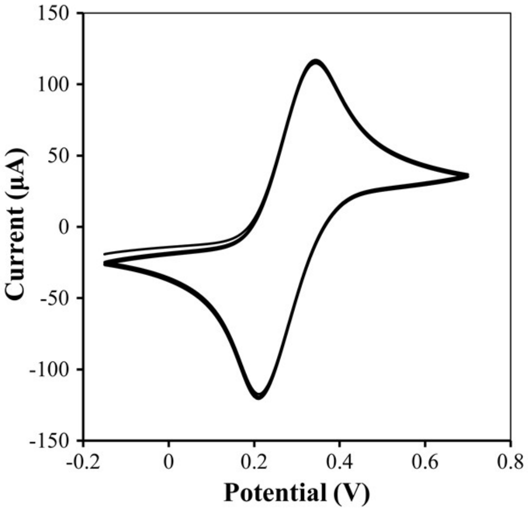

Fig. s6 Cyclic voltammetry of the NiO@Ni-His-GQD double heterojunction/GCE in the PBS of 7.0 containing 5.0 mM [Fe(CN)$_6$]$^{4-}$

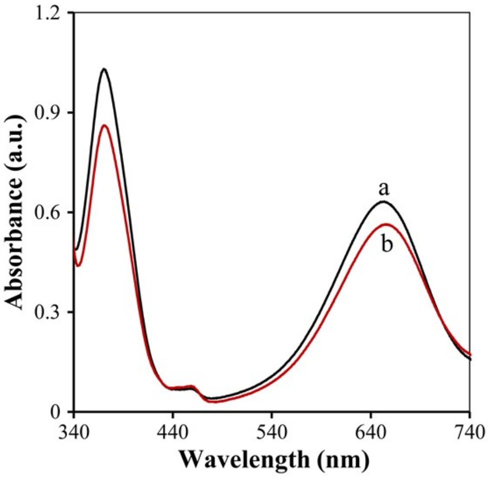

Fig. s7 Absorption spectra of the reaction system containing NiO@Ni-His-GQD+TMB (a) and NiO@Ni-His-GQD gel tablet+TMB (b)

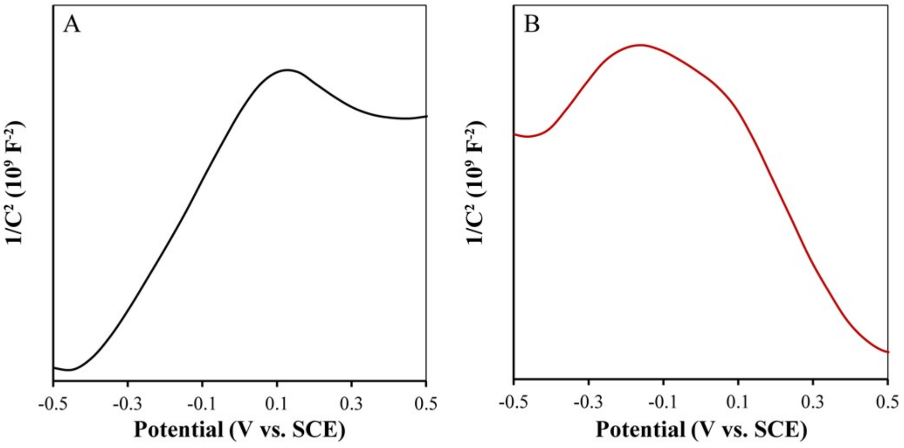

Fig. s8 The Mott-Schottky plots of His-GQD and His-GQD-B

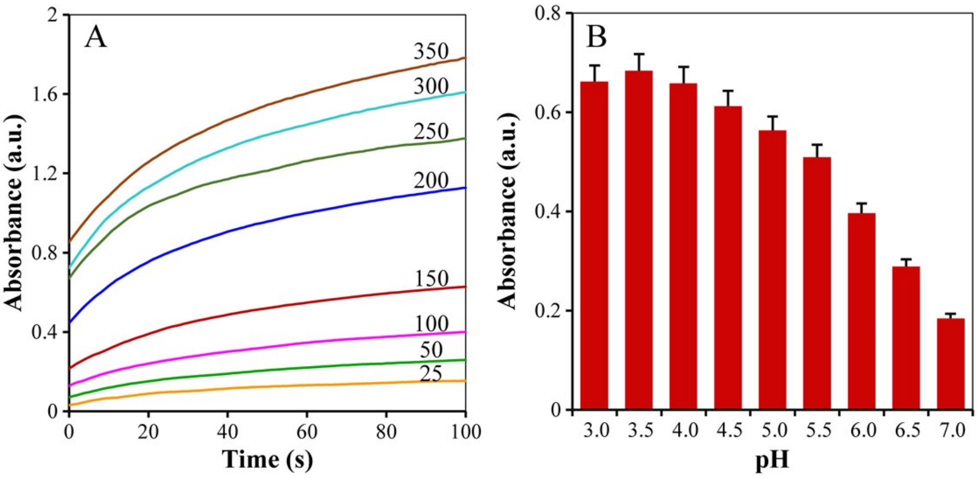

Fig. s9 Effects of NiO@Ni-His-GQD concentration and reaction time (A), pH (B) on the oxidase-like activity of NiO@Ni-His-GQD

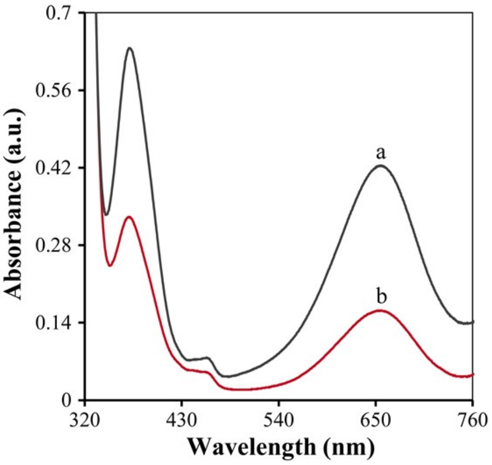

Fig. s10 Absorption spectra of NiO@Ni-His-GQD+TMB in the absence (a) and presence (b) of lambda-cyhalothrin

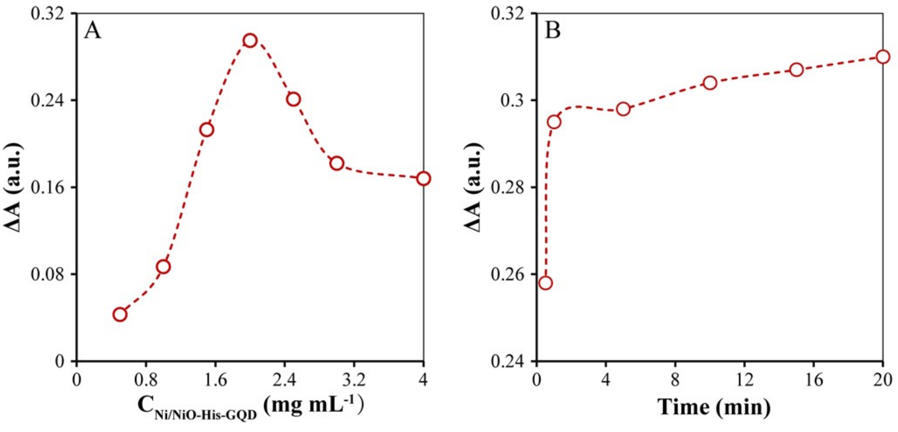

Fig. s11 Relationship curves of the concentration of NiO@Ni-His-GQD (A) in NiO@Ni-His-GQD gel tablet and coloration time (B) with the ΔA value caused by lambda-cyhalothrin

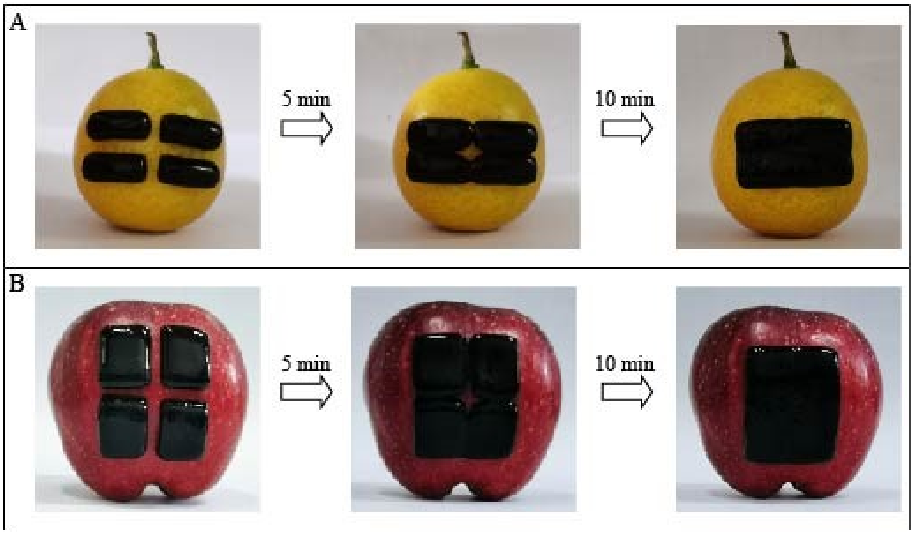

Fig. s12 Self-healing experiments of NiO@Ni-His-GQD gel on the surface of kumquat and apple

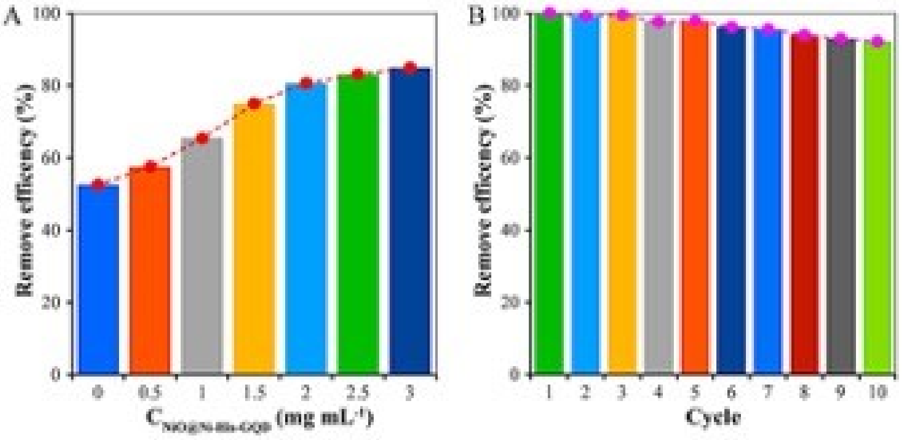

Fig. s13 The removal efficiency obtained by using different gel with different concentration of NiO@Ni-His-GQD (A) and the retention values obtained by using the same gel for different times (B)

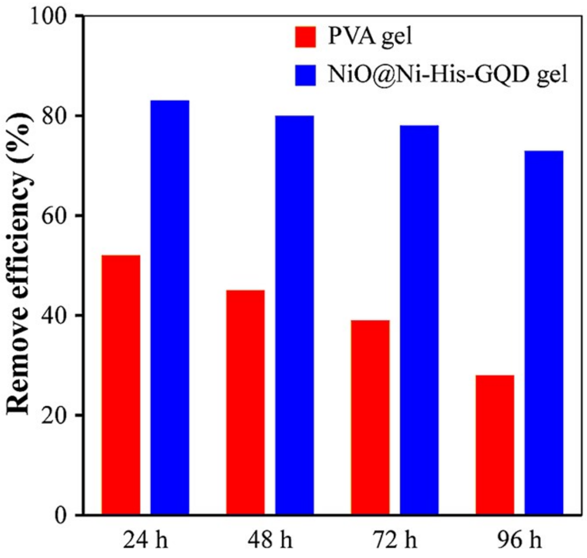

Fig. s14 The removal efficiency of lambda-cyhalothrin on kumquat surface for different time using PVA gel and NiO@Ni-His-GQD gel

Reference：

1. L. Liu, R.Y. Li, T. Lai, Z.J. Li, Z.G. Gu, His-CDs@NaTbF$_4$: Synthesis and Application in Detection of Histidine and Cancer Cell Imaging, Chinese J. Inorg. Chem. 34 (2018) 1240-1248, https://doi.org/10.11862/CJIC.2018.154.

2. G.S. Guo, D.H. Zheng, Z.H. Wang, J.H. Lu, H.Y. Guo, Preparation of NiO nanoparticles by homogeneous precipitation method and its characterization, Journal of Beijing university of chemical technology 31 (3) (2004) 74-76+81, https://doi.org/10.13543/j.cnki.bhxbzr.2004.03.019.

3. Y.L. Dong, H.G. Zhang, Z.U. Rahman, L. Su, X.J. Chen, J. Hu, X.G. Chen, Graphene oxide–Fe$_3$O$_4$ magnetic nanocomposites with peroxidase-like activity for colorimetric detection of glucose, Nanoscale 4 (2012) 3969-3976, https://doi.org/10.1039/c2nr12109c.